OPEN

CHARACTERISTICS OF THE FOVEAL MICROVASCULATURE IN CHILDREN WITH MARFAN SYNDROME

An Optical Coherence Tomography Angiography Study

HUI CHEN, PHD, KIT YEE NG, MD, SONGSHAN LI, PHD, GUANGMING JIN, PHD, QIANZHONG CAO, PHD, ZHANGKAI LIAN, MD, XIAOLING LUO, BS, XIAOYAN DING, PHD, DANYING ZHENG, MD

Purpose: To investigate the characteristics of foveal microvasculature in children with Marfan syndrome (MFS).

Methods: Ninety eyes from 45 MFS patients and 76 eyes from 38 healthy individuals of age-matched, sex-matched, and axial length-matched were enrolled. Characteristics of the superficial capillary plexus including the vessel density, perfusion density, and foveal avascular zone were analyzed by optical coherence tomography angiography.

Results: The vessel density and the circularity index of the foveal avascular zone were significantly decreased in the MFS group compared with the controls ($P = 0.017$ and $P = 0.004$ respectively). In MFS group, the central vessel density ($P = 0.003$) and perfusion density ($P = 0.001$) were negatively correlated with the best-corrected visual acuity. The foveal avascular zone area was correlated with the aortic diameters ($P = 0.001$) and the paratemporal perfusion density was correlated with the ejection fraction ($P = 0.003$). Moreover, the paratemporal perfusion density and the circularity index of foveal avascular zone were found to be correlated with the aortic Z-score ($P < 0.001$ and $P = 0.003$ respectively).

Conclusion: Retinal microvascular decrease and its correlation with best-corrected visual acuity and cardiac functions were observed in the MFS group. The optical coherence tomography angiography may help to characterize the underlying pathophysiology features of MFS and enable early detection and prevention of vascular changes in MFS.

RETINA 42:138–151, 2022

Marfan syndrome (MFS) is an autosomal dominant disease that affects the connective tissue. It was estimated that in every 100,000 people, 2 to 3 individuals are suffering from MFS.[1] Marfan syndrome is caused by a mutation in the gene that codes fibrillin-1 (FBN1), which is associated with several skeletal and vascular abnormalities, and a varied range of ocular manifestations, including ectopia lentis (EL).[2]

Fibrillin-1 is the most abundant elastic microfibril present in human eyes. Fibrillin-1 can also be found in vascular smooth muscle cells and vascular endothelium contributing to regulation of blood flow. In the systemic circulation, structural cardiovascular abnormalities such as aortic dilation are the primary complication in MFS.[3] However, the mechanism of how FBN1 regulates the microvascular blood flow in the retinal vascular system is not well understood.

As we all know, the branch of the internal carotid artery, ophthalmic artery supplies blood to the eye, therefore, perturbations in the coronary macrocirculation and microcirculation, in addition to genetic predisposition, can be reflected by the retinal microvasculature. Moreover, microvascular endothelial dysfunction is an early event in the development of cardiovascular disease and assessment of retinal microvasculature provides valuable information that helps to determine the health of endothelium. In particular, optical coherence tomography angiography (OCTA) visualizes the retinal blood vessel and evaluates the retinal microvasculature in a noninvasive

manner.[4] Retinal fundus images are used in the detection of subtle, early microvascular variation, prediction, and examination of the target organ damage in vascular diseases.[5]

Little is known about the characteristics of foveal microvasculature in the eyes of patients with MFS. Detailed images of retinal vascular layers are required to understand the association between retinal microvascular changes and MFS. In this study, we investigated different parameters of macular microcirculation in children with MFS including foveal avascular zone (FAZ) parameters, macular vessel density (VD), and perfusion density (PD) based on OCTA. These parameters of the eyes in the MFS group were compared with age-, sex-, and axial length (AL)-matched control eyes, and their correlation with other clinical functional or structural data such as best-corrected visual acuity (BCVA), OCT indices, degrees of ectopia lentis (EL), aortic size, Z-score, and ejection fraction (EF) were analyzed.

Methods

Patients

This cross-sectional observational study was conducted in Zhongshan Ophthalmic Center over 6 months in the period from August 2019 to August 2020.

The study was approved by the Ethical Committee of Zhongshan Ophthalmic Center. The research followed the tenets of the Declaration of Helsinki. Informed consent was obtained from all 18-year-old patients or from the legal guardian for those who were less than 18 years old.

Eighty-eight patients consented to the study. Fifty patients with proven MFS according to Ghent-2 criteria and aged between 5 and 18 years were included in this study. Only eyes with AL between 21.0 mm and 26.0 mm were included. Healthy subjects were matched for age, sex, and AL, and then included as controls. Patients with retinal detachments repaired with a scleral buckle, known glaucoma or other retinal diseases were excluded from this study. Patients with ocular surface disorders such as corneal opacity or severe dryness that affect the OCTA image quality were also excluded from this study.

All patients undertook a routine ocular examination, including BCVA, (expressed as logarithm of the minimum angle of resolution [logMAR] units), slit-lamp biomicroscopy, noncontact tonometer, indirect ophthalmoscopy and AL measurement (IOL Master, Carl Zeiss Meditec, Jena, Germany), 1% tropicamide with 2.5% phenylephrine, or 1% cyclopentolate were used for all patients. For the calculation of the spherical equivalent (SE), we used only phakic or pseudophakic eyes. We also excluded phakic eyes with severe EL requiring aphakic correction. Spherical equivalent was calculated as the sum of the spherical plus half of the cylindrical error. Owing to insufficient signal strength, 5 of 50 patients were excluded for macular data. The degree of EL was classified into three broad groups according to previous reference.[6]

Optical Coherence Tomography Measurements

Cirrus HD-OCT instrument (Carl Zeiss Meditec, Dublin, CA) was used to perform SD-OCT imaging. A total diameter of 6 mm from nine subfield areas of the Early Treatment Diabetic Retinopathy Study was quantified by a macular cube scan. Central macular thickness (CMT) refers to the thickness of the central 1-mm diameter. The macular cube in a 512 × 128 combination mode of scan was used to measure the CMT. The ganglion cell-inner plexiform layer thickness was determined using the ganglion cell analysis algorithm. We analyzed the retinal nerve fiber layer (RNFL), CMT and the average thickness of macular ganglion cell-inner plexiform layer.

Optical Coherence Tomography Angiography Measurements

Optical coherence tomography angiography (Cirrus AngioPlex 5000 software V.10.0, Carl Zeiss Meditec, Dubin, CA) with a scanning mode of 3 × 3 mm was used to acquire images for all subjects. All subjects were scanned at the first visit or 3 months after surgery when the inflammation had resolved. Scans with significant artefacts (such as large floaters, segmentation errors, and blinking or motion artefact) or signal strength lower than eight were excluded.[7]

This study analyzed the superficial capillary plexus. The superficial capillary plexus was autosegmented by the built-in software (AngioPlex, V.10.0). Image segmentation of superficial capillary plexus was

From the State Key Laboratory of Ophthalmology, Zhongshan Ophthalmic Center, Sun Yat-sen University, Guangzhou, China.

Supported by the National Natural Science Foundation of China (81873673, 81970813 and 81900841).

None of the authors has any conflicting interests to disclose.

H. Chen AND K. Y. Ng authors contributed equally to this work.

Reprint requests: Danying Zheng, MD, State Key Laboratory of Ophthalmology, Zhongshan Ophthalmic Center, Sun Yat-sen University, 54 South Xianlie Road, Guangzhou, 510060, China; e-mail: zhengdyy@163.com

assessed and manually adjusted to reduce the segmentation errors.

The superficial retinal layer was imaged from the internal limiting membranes of the retina to the inner plexiform layer. In this study, the central foveal area is defined as the small circle 1 mm in diameter and centered at the fovea; the foveal area is defined as the large circle with 3 mm in diameter and centered at the fovea; and the parafoveal area is defined as the annular area in which the large circle without the small central circle. The inner ring was further divided into 4 equal quadrants (superior, inferior, nasal, and temporal) for subregion analysis (Figure 1). The VD is defined as the sum of the length of vessels in a particular area, and it is shown as mm^{-1} including whole fovea superficial capillary VD, central foveal superficial VD, and parafoveal superficial VD. The PD is defined as the percentage of the area occupied by the vessels in a particular area, and it is shown as mm^2/mm^2 including whole fovea superficial capillary PD, central foveal superficial PD, and parafoveal superficial PD. The center of the FAZ was also detected including the FAZ area, FAZ perimeter, and FAZ circularity index (CI). The OCTA data were acquired by the software automatically (AngioPlex, version 10.0). The BCVA and refraction data of all participants were recorded. All the examinations in this study were performed by one experienced technician using the same machine.

Echocardiography

Patients in the MFS group were examined with a full ultrasound system (Philips EnVisor C-HD; Philips Co, Best, The Netherlands) at baseline for a complete echocardiographic study. Aortic root diameters and left ventricular EF were measured following the current guidelines.[8] The parasternal long-axis view was used to acquire aortic measurements. The aortic root was measured from the largest diameter within the sinuses of Valsalva. All echocardiographic images were acquired and analyzed by a single observer in a blinded manner. Aortic Z-score was calculated using the Colan formula[9] according to recommendations of the Marfan Foundation. Aortic Z-score with correction for body height was used in the regression analysis because of its best clinical performance.[10]

Statistical Analysis

All the numerical information was statistical analyzed by the SPSS version 22.0 (SPSS, Chicago, IL). The Kolmogorov–Smirnov test of normality was used. The differences of demographic characteristics and OCTA parameters between MFS group and healthy group were analyzed using the generalized estimating equation analysis. The correlation between the OCTA measurements and other clinical, functional, or structural data was analyzed. Each OCTA measurement was analyzed independently from the other measurements. Areas under the receiver operating characteristics curves (AUCs) were calculated and assessed as described previously.[11] The desired overall α level was 0.05; when multiple outcomes were compared between the groups, the α level was adjusted through Bonferroni's correction.

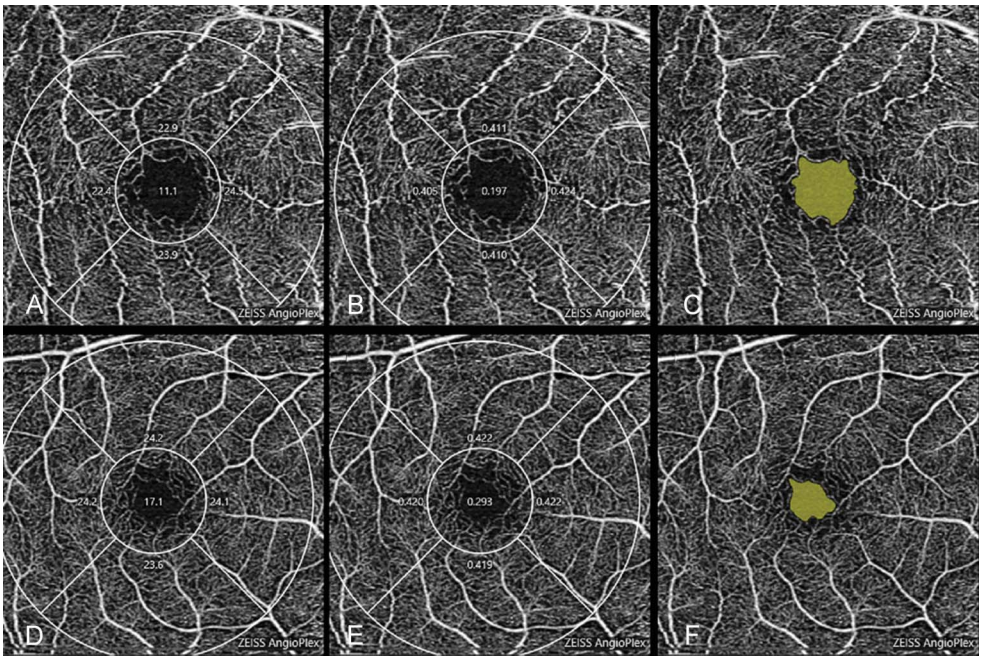

Fig. 1. A representative OCTA image (**A**–**C**) of a 5-year-old boy with Marfan syndrome and a 11-year-old healthy boy (**D**–**F**). The vessel densities for the total area of the two participants were 22 mm^{-1} (**A**) and 23.3 mm^{-1} (**D**), and the perfusion densities were 0.338 (**B**) and 0.406 (**E**), respectively. The automatically detected foveal avascular zone areas were 0.26 mm^2 (**C**) and 0.11 mm^2 (**F**), respectively.

Results

Baseline and Demographic Data

Clinical characteristics of participants are summarized in Table 1. A total of 90 eyes from 45 MFS patients (25 men and 20 women) from 5 to 18 years old (mean 8.38 ± 3.55 years) were investigated. Seventy-six eyes of age- and sex-matched, healthy participants (20 men and 18 women, aged 7.97 ± 2.14 years) were also included in this study as control subjects. The AL was 24.74 ± 1.97 mm in the MFS group and 24.29 ± 1.35 mm in the control group (P = 0.366). The age, sex distribution, intraocular pressure (IOP), refractive error, and AL were similar in both groups. We confirmed the significant difference between the BCVA (logMAR [Snellen]) of MFS groups and healthy controls (0.31 ± 0.26 [20/41] vs. 0.00 ± 0.02 [20/20], P = 0.009).

Retinal Nerve Fiber Layer, Central Macular Thickness and Ganglion Cell-Inner Plexiform Layer Thickness

The MFS patients had 98.24 ± 11.98 μm RNFL, 244.5 ± 10.13 μm CMT, and 80.48 ± 10.86 μm ganglion cell-inner plexiform layer thickness, which were all relatively thinner than the controls (100.94 ± 8.61 μm in RNFL, 252.78 ± 14.40 μm in CMT, 83.29 ± 5.74 μm in ganglion cell-inner plexiform layer thickness) although with no statistical difference (P = 0.092, P = 0.096, P = 0.236, respectively, Table 2).

Vessel Density

The full superficial foveal VD was 20.29 ± 2.27 mm^{-1} in the MFS group, which was confirmed significantly lower than those in healthy group by mixed factorial analysis (21.79 ± 0.99 mm^{-1}, P = 0.017, Table 3). The VD of parafoveal, nasal, and inferior values in the inner ring in MFS patients were 21.40 ± 2.26 mm^{-1}, 21.48 ± 2.59 mm^{-1} and 21.13 ± 2.72 mm^{-1}, which were lower than that in the normal controls, although these were not significantly different after multivariate analysis.

Perfusion Density

The central superficial PD of MFS group (0.20 ± 0.06) was lower than that in the healthy group (0.23 ± 0.05) although these were not significantly different after multivariate analysis (Table 2).

Foveal Avascular Zone Characteristics

The CI of FAZ in patients with MFS (0.64 ± 0.11) was significantly higher than in the healthy controls (0.70 ± 0.08, P = 0.004) (Table 3).

Correlation Between Optical Coherence Tomography Angiography Indices and Other Clinical Functional or Structural Data

The correlations between the OCTA parameters and other parameters in MFS group, including age, gender,

Table 1. Clinical and Demographic Characteristics of Patients With MFS and Healthy Control Subjects

Descriptive	Patients	Control	*P*
Eyes, n	90 (45)	76 (38)	—
Age, years			
Mean ± SD	8.38 ± 3.548	7.97 ± 2.14	0.352
Range	5–18	5–18	
Sex			
Male, n (%)	25 (55.6%)	20 (52.6%)	0.095
BCVA (logMAR [Snellen])	0.31 ± 0.26 (20/41)	0.00 ± 0.02 (20/20)	0.009*
IOP, mmHg	11.92 ± 2.90	13.10 ± 2.87	0.914
AL, mm	24.74 ± 1.97	24.29 ± 1.35	0.366
SE, diopter	−1.69 ± 6.21	−1.69 ± 2.30	0.451
Aortic diameter (sinuses of Valsalva, mm)	23.90 ± 5.64	—	
Aortic Z-score	1.57 ± 2.00	—	
Aortic Z-score≥2 (%)	25 (34%)	—	
Aortic Z-score≥3 (%)	16 (22%)	—	
Ejection fraction (%)	68.53 ± 5.88	—	
Degree of lens dislocation (%)			
Mild	0 (0)	—	
Moderate	9 (5%)	—	
Severe	90 (52%)	—	

Data are presented as the mean ± SD.
*P value < 0.05.

Table 2. Quantitative Analysis Results of the Vascular and Structure Parameters in Patients With MFS and Normal Controls

	Patients	Control
VD, mm^{-1}		
Full area	20.29 ± 2.27	21.79 ± 0.99
Central area	11.56 ± 3.31	13.35 ± 2.77
Para	21.40 ± 2.26	22.88 ± 0.95
Inner ring		
Nasal	21.48 ± 2.59	23.03 ± 1.04
Temporal	21.42 ± 2.46	22.71 ± 1.06
Superior	21.48 ± 2.46	22.97 ± 1.15
Inferior	21.13 ± 2.72	22.80 ± 1.30
Perfusion density		
Full area	0.37 ± 0.04	0.38 ± 0.02
Central area	0.20 ± 0.06	0.23 ± 0.05
Para	0.39 ± 0.07	0.40 ± 0.01
Inner ring		
Nasal	0.39 ± 0.05	0.40 ± 0.02
Temporal	0.39 ± 0.04	0.40 ± 0.02
Superior	0.39 ± 0.04	0.41 ± 0.02
Inferior	0.38 ± 0.05	0.40 ± 0.02
FAZ		
Area, mm^2	0.25 ± 0.08	0.21 ± 0.10
Perimeter, mm	2.20 ± 0.48	1.91 ± 0.45
Circularity index	0.64 ± 0.11	0.70 ± 0.08
RNFL, μm		
Average	98.24 ± 11.98	100.94 ± 8.61
Superior	113.52 ± 23.41	124.28 ± 15.32
Inferior	129.88 ± 18.28	128.82 ± 14.95
CMT, μm	244.54 ± 10.13	252.78 ± 14.40
Ganglion cell layer thickness, μm	80.48 ± 10.86	83.29 ± 5.74
Vertical C/D ratio	0.38 ± 0.17	0.41 ± 0.19

Data are presented as the mean ± SD.

BCVA, IOP, AL, degrees of EL, aortic diameters, Z-scores, and EF, are listed in Tables 4–6.

The central VD ($\beta = 0.088$, $P < 0.001$) and central PD ($\beta = 0.001$, $P = 0.001$) were found to positively correlate with the CMT. The central VD ($\beta = -3.248$, $P = 0.003$) and PD ($\beta = -0.061$, $P = 0.001$) were also found to negatively correlate with BCVA.

Moreover, the FAZ area were correlated with the aortic diameters (sinuses of Valsalva) ($\beta = -0.011$, $P = 0.001$). The paratemporal PD and the CI of FAZ were all correlated with the Z-score ($\beta = 0.020$, $P < 0.001$; $\beta = 0.039$, $P = 0.003$). The paratemporal PD were also found to be correlated with EF ($\beta = 0.002$, $P = 0.003$). In addition, lower paratemporal VD and PD were both found to be significantly associated with male sex and decrease central VD and PD were also found to be correlated with longer AL (all $P < 0.003$).

Diagnostic Ability of Vessel Density and Perfusion Density

The AUCs of VD and PD in various locations are presented in Figure 2. Para-area VD showed the best diagnostic performance with AUC of 0.770 followed by full-area VD (AUC: 0.760) and parainferior area VD (AUC: 0.750).

Discussion

Marfan syndrome is mostly caused by mutations in genes controlling the synthesis of FBN1. Large-vessel arterial complications in patients with MFS were well described. In MFS patients, leaky heart valves impairs forward flow of blood and can induce structural modifications of the arterial wall and reduces vessel wall compliance. Specific MFS cases with aneurysm formation have been reported, suggesting that small arteries may be affected in this disorder.[12] Therefore, patients with MFS may have changes in the vessel wall of microvasculature.

The retina is one of the end organs that shares many vascular, structural, and physiological properties with the cerebral and coronary circulations.[11] Moreover, retinal vessels are easily accessible compared with other end organs offering direct access for evaluation of the microvasculature. Optical coherence

Table 3. Retinal Vascular Parameter Differences Between MFS Versus Control Subjects by Univariate and Multivariate Logistic Regression Analysis

	Full-Area VD				Full-Area PD	
	Univariate		Multivariate		Univariate	
	β (95% CI)	*P*	β (95% CI)	*P*	β (95% CI)	*P*
MFS vs. control	−1.692 (−2.426 to −0.959)	0.000	−1.020 (−1.853 to −0.186)	**0.017***	−0.021 (−0.033 to −0.009)	0.001
Age, years	−0.102 (−0.266 to 0.063)	0.226			−0.002 (−0.005 to 0.001)	0.142
Sex (male/female)	−1.017 (−1.859 to −0.175)	0.018	−0.898 (−1.667 to −0.130)	0.022	−0.015 (0.028 to −0.002)	0.023
BCVA (logMAR [snellen])	−4.013 (−6.813 to −1.212)	0.005	−2.607 (−6.451 to 1.236)	0.184	−0.059 (−0.105 to −0.012)	0.014
SE, diopter)	0.041 (−0.073 to 0.155)	0.479			0.000 (−0.001 to 0.002)	0.648
Intraocular pressure, mmHg	0.071 (−0.009 to 0.151)	0.082			0.001 (5.904E-5 to 0.002)	0.039
AL, mm	0.246 (−0.150 to 0.642)	0.224			0.002 (−0.005 to 0.008)	0.616
CMT, μm	0.031 (0.014 to 0.048)	0.000	0.016 (0.002 to 0.031)	0.026	0.000 (0.000 to 0.001)	0.001
Ganglion cell layer, μm	0.043 (−0.061 to 0.147)	0.420			0.001 (−0.001 to 0.003)	0.369
Average RNFL, μm	−0.020 (−0.015 to 0.056)	0.265			0.000 (0.000 to 0.001)	0.451
Inferior RNFL, μm	0.008 (−0.013 to 0.029)	0.471			0.000 (0.000 to 0.000)	0.327
Superior RNFL, μm	0.016 (−0.006 to 0.037)	0.165			0.000 (0.000 to 0.000)	0.503
vCD (%)	−0.991 (−3.738 to 1.755)	0.479			−0.991 (−3.738 to 1.755)	0.479

	Full-Area PD		FAZ Circularity Index			
	Multivariate		Univariate		Multivariate	
	β (95% CI)	*P*	β (95% CI)	*P*	β (95% CI)	*P*
MFS vs. control	−0.010 (−0.023 to −0.004)	0.172	−0.068 (−0.101 to −0.035)	0.000	−0.054 (−0.091 to −0.017)	**0.004***
Age, years			−0.002 (−0.006 to 0.002)	0.368		
Sex (male/female)	−0.013 (−0.026 to −0.001)	0.041	0.006 (−0.030 to 0.043)	0.740		

(*continued on next page*)

Table 3. (*Continued*)

	Full-Area PD		FAZ Circularity Index			
	Multivariate		Univariate		Multivariate	
	β (95% CI)	*P*	β (95% CI)	*P*	β (95% CI)	*P*
BCVA (logMAR [snellen])	−0.047 (−0.112 to 0.018)	0.155	−0.118 (−0.192 to −0.044)	0.002	−0.035 (−0.111 to 0.040)	0.359
SE, diopter)			−0.003 (−0.006 to 0.001)	0.185		
Intraocular pressure, mmHg	0.001 (−0.001 to 0.002)	0.300	0.006 (0.001 to 0.012)	0.022	0.005 (0.000 to 0.010)	0.032
AL, mm			0.011 (−0.003 to 0.025)	0.111		
CMT, μm	0.000 (−3.300E-5 to 0.000)	0.067	0.000 (−0.001 to 0.001)	0.805		
Ganglion cell layer, μm			0.000 (−0.002 to 0.003)	0.753		
Average RNFL, μm			0.000 (−0.002 to 0.001)	0.640		
Inferior RNFL, μm			−0.001 (−0.002 to 5.816E-5)	0.063		
Superior RNFL, μm			6.250E-5 (−0.001 to 0.001)	0.897		
vCD (%)			−0.087 (−0.448 to 0.751)	0.103		

**P* value significant after applying the corrected alpha threshold of 0.017; Bold indicates significant values.

Table 4. Correlations Between Baseline Characteristics and Vascular Density in MFS Patients Using Generalized Estimating Equations for Logistic Regression Analysis

	Central VD		Para-Area VD		Full-Area VD		Para-Nasal-Area VD
	β (95% CI)	*P*	β (95% CI)	*P*	β (95% CI)	*P*	β (95% CI)
Age, years	−0.660 (−0.971 to −0.355)	<**0.001***	0.151 (−0.146 to 0.448)	0.320	0.060 (−0.232 to 0.352)	0.686	0.159 (−0.253 to 0.570)
Sex (male %)	−1.650 (−3.182 to −0.120)	0.035	−2.196 (−3.607 to −0.784)	**0.002***	−2.144 (−3.545 to −0.743)	**0.003***	−2.793 (−4.771 to −0.815)
BCVA (logMAR [Snellen])	−3.248 (−5.426 to 1.070)	**0.003***	−0.973 (−2.685 to 0.738)	0.265	−1.230 (−2.920 to 0.461)	0.154	−1.970 (−4.685 to 0.744)
SE, D	−0.048 (−0.146 to 0.049)	0.329	−0.062 (−0.139 to 0.015)	0.113	−0.059 (−0.136 to 0.019)	0.137	−0.130 (−0.255 to −0.005)
Intraocular pressure, mmHg	−0.080 (−0.265 to 0.105)	0.396	0.023 (−0.151 to 0.198)	0.794	0.018 (−0.153 to 0.189)	0.839	0.111 (−0.097 to 0.319)
AL, mm	0.709 (0.381 to 1.037)	<**0.001***	0.057 (−0.243 to 0.357)	0.710	0.131 (−0.165 to 0.428)	0.384	0.178 (−0.259 to 0.616)
CMT, μm	0.088 (0.046 to 0.130)	<**0.001***	−0.005 (−0.038 to 0.028)	0.768	0.006 (−0.028 to 0.040)	0.740	−0.041 (−0.097 to 0.016)
Ganglion cell layer, μm	0.070 (−0.043 to 0.182)	0.227	0.087 (−0.046 to 0.219)	0.201	0.086 (−0.046 to 0.218)	0.201	0.075 (−0.074 to 0.224)
vCD (%)	1.583 (−2.110 to 5.276)	0.401	−1.247 (−3.735 to 1.242)	0.326	−0.983 (−3.475 to 1.509)	0.440	−0.181 (−4.105 to 3.744)
Average RNFL, μm	−0.053 (−0.167 to 0.060)	0.359	0.029 (−0.077 to 0.135)	0.593	0.021 (−0.079 to 0.121)	0.682	0.071 (−0.055 to 0.197)
Superior RNFL, μm	0.023 (−0.025 to 0.072)	0.347	−0.011 (−0.048 to 0.026)	0.577	−0.007 (−0.043 to 0.029)	0.714	−0.014 (−0.059 to 0.031)
Inferior RNFL, μm	0.050 (−0.010 to 0.110)	0.100	0.012 (−0.046 to 0.070)	0.680	0.015 (−0.040 to 0.070)	0.588	0.002 (−0.062 to 0.065)
Degree of lens dislocation (%) (severe)	1.859 (−1.980 to 5.697)	0.343	−0.731 (−3.985 to 2.522)	0.660	−0.393 (−3.470 to 2.685)	0.803	0.563 (−4.681 to 5.807)
Aortic diameter sinuses of Valsalva, mm	0.200 (−0.085 to 0.486)	0.169	−0.232 (−0.513 to 0.049)	0.105	−0.187 (−0.466 to 0.092)	0.188	−0.202 (−0.546 to 0.143)
Z score	−0.150 (−0.880 to 0.580)	0.687	0.723 (−0.040 to 1.486)	0.063	0.632 (−0.125 to 1.389)	0.102	0.493 (−0.378 to 1.364)
EF	0.089 (−0.018 to 0.197)	0.103	0.09 (0.003 to 0.117)	0.042	0.094 (0.006 to 0.182)	0.036	0.076 (−0.028 to 0.180)

	Para-Nasal-Area VD	Para-Temporal-Area VD		Para-Superior-Area VD		Para-Inferior-Area VD	
	P	β (95% CI)	*P*	β (95% CI)	*P*	β (95% CI)	*P*
Age, years	0.450	0.047 (−0.263 to 0.357)	0.766	0.157 (−0.190 to 0.505)	0.375	0.105 (−0.239 to 0.450)	0.549
Sex (male %)	0.006	−2.211 (−3.566 to −0.857)	**0.001***	−1.873 (−3.504 to −0.241)	0.024	−1.676 (−3.547 to 0.196)	0.079
BCVA (logMAR [Snellen])	0.155	−1.046 (−2.907 to 0.815)	0.271	−0.341 (−2.501 to 1.819)	0.757	−2.161 (−4.428 to 0.106)	0.062
SE, D	0.041*	−0.079 (−0.160 to 0.002)	0.056	−0.117 (−0.243 to 0.008)	0.067	0.007 (−0.080 to 0.094)	0.866
Intraocular pressure, mmHg	0.295	0.026 (−0.148 to 0.200)	0.769	0.009 (−0.211 to 0.229)	0.936	−0.052 (−0.256 to 0.152)	0.616
AL, mm	0.425	−0.010 (−0.293 to 0.272)	0.942	0.126 (−0.237 to 0.488)	0.497	−0.121 (−0.472 to 0.231)	0.501
CMT, μm	0.156	−0.022 (−0.059 to 0.015)	0.244	0.020 (−0.029 to 0.069)	0.430	−0.021 (−0.066 to 0.025)	0.376
Ganglion cell layer, μm	0.322	0.091 (−0.025 to 0.207)	0.125	0.108 (−0.011 to 0.228)	0.076	0.082 (−0.079 to 0.243)	0.318

(*continued on next page*)

Table 4. (*Continued*)

	Para-Nasal-Area VD	Para-Temporal-Area VD		Para-Superior-Area VD		Para-Inferior-Area VD	
	P	β (95% CI)	*P*	β (95% CI)	*P*	β (95% CI)	*P*
vCD (%)	0.928	−1.504 (−4.433 to 1.426)	0.314	−2.153 (−5.944 to 1.638)	0.266	−2.257 (−6.048 to 1.534)	0.243
Average RNFL, μm	0.268	−0.003 (−0.095 to 0.088)	0.944	0.041 (−0.096 to 0.178)	0.562	0.000 (−0.135 to 0.134)	0.995
Superior RNFL, μm	0.544	−0.002 (−0.034 to 0.030)	0.909	−0.021 (−0.068 to 0.026)	0.375	−0.007 (−0.050 to 0.036)	0.748
Inferior RNFL, μm	0.959	0.038 (−0.021 to 0.097)	0.204	−0.005 (−0.073 to 0.063)	0.880	0.035 (−0.033 to 0.102)	0.311
Degree of lens dislocation (%) (severe)	0.833	−3.042 (−7.566 to 1.483)	0.188	−3.533 (−8.984 to 1.918)	0.204	1.300 (−2.925 to 5.524)	0.547
Aortic diameter sinuses of Valsalva, mm	0.817	−0.205 (−0.468 to 0.058)	0.126	−0.241 (−0.555 to 0.073)	0.133	−0.182 (−0.499 to 0.135)	0.260
Z score	0.267	0.899 (0.207 to 1.590)	0.011	0.724 (−0.046 to 1.494)	0.066	0.586 (−0.303 to 1.474)	0.196
EF	0.154	0.132 (0.041 to 0.223)	0.004	0.073 (−0.029 to 0.175)	0.162	0.062 (−0.037 to 0.161)	0.217

**P* value significant after applying the corrected alpha threshold of 0.003. Bold indicates significant values.

tomography angiography is a novel technique that requires no-dye examination and can generate depth-resolved imaging of capillary in the foveal retina from three dimensions. In this study, we used OCTA to compare the microvascular structure including FAZ, VD, and PD between MFS and control group.

The results of current study showed that the full superficial retinal VD and the CI of FAZ were reduced in MFS group than those of the control group. Several factors contribute to changes in vessel flow of MFS patients. Fibrillin-1 serves as structural components of elastic and inelastic microfibrils, which support the connective tissue. Mutations in FBN1 may impair the normal structural and functional properties of FBN1 and further affect the connective tissue. In MFS patients, the architecture of connective tissue in the vessel wall was damaged, which may contribute to reduced blood flow. In addition, FBN1 can reduce the hemodynamic burden and parietal stress together with the fibers, prevent over-distension of elastin, improve arterial elasticity, and support flow-mediated vasodilation.[13] Fibrillin-1 also regulates the release of transforming growth factor-β, which may lead to increased wall thickness, fragmentation, and disarray of elastic fibers and subsequently increased collagen deposition. We previously reported that the level of transforming growth factor-β in aqueous humor was increased in MFS patients.[14] Moreover, in the vascular endothelium of MFS patients, endothelial dysfunction induced by dysfunctional FBN1 may lead to decreased vessel flow in foveal.[15] It is hypothesized that FBN1 coordinates the endothelial cytoskeletal network and the structural components of the extracellular matrix and thus regulates the blood flow.

In addition, our study showed that the FAZ area was correlated with the aortic diameters and the paratemporal PD was correlated with the left ventricular EF; the paratemporal PD and the CI of FAZ were also found to be correlated with the aortic Z-score. These echocardiographic parameters are known to represent sensible biomarkers of left ventricular diastolic dysfunction and left ventricular diastolic filling pressure, an early index of myocardial damage. Patients with MFS can show frequent cardiovascular hemodynamic changes including mitral valve prolapse and aortic dilatation. The superficial retinal microvasculature was believed to be closely related to arterial blood circulation. Abnormal functions in aorta pressure, flow waves, and arterial stiffness have been found in pediatric MFS patients.[16] Echocardiographic studies on MFS patients also showed that the pattern of transmittal diastolic flow was abnormal.[17] A previous study found that aortic root diameter was correlated with left ventricular dysfunction and flow-mediated endothelial

Table 5. Correlations Between Baseline Characteristics and Perfusion Density in MFS Patients Using Generalized Estimating Equations for Logistic Regression Analysis

	Central PD		Parafoveal PD		Full-Area PD		Paranasal-Area PD	
	β (95% CI)	*P*	β (95% CI)	*P*	β (95% CI)	*P*	β (95% CI)	*P*
Age, years	−0.013 (−0.018 to −0.008)	**<0.001***	0.003 (−0.002 to 0.007)	0.195	0.001 (−0.003 to 0.006)	0.615	0.004 (−0.003 to 0.010)	0.281
Sex (male%)	−0.024 (−0.002 to 0.007)	0.078	−0.029 (−0.052 to −0.007)	0.011	−0.029 (−0.051 to −0.006)	0.013	−0.04 (−0.072 to −0.008)	0.013
BCVA (logMAR [Snellen])	−0.061 (−0.052 to −0.007)	**0.001***	−0.018 (−0.042 to 0.007)	0.155	−0.023 (−0.048 to 0.001)	0.065	−0.039 (−0.081 to 0.002)	0.064
SE, D	−0.001 (−0.042 to 0.007)	0.310	−0.001 (−0.002 to 3.393E-5)	0.058	−0.001 (−0.002 to 8.205E-5)	0.071	−0.002 (−0.004 to −0.001)	0.005
Intraocular pressure, mmHg	−0.001 (−0.002 to 3.393E-5)	0.404	0.001 (−0.002 to 0.004)	0.546	0.001 (−0.002 to 0.003)	0.675	0.002 (−0.001 to 0.006)	0.179
AL, mm	0.009 (−0.002 to 0.004)	**0.001***	−0.001 (−0.006 to 0.003)	0.582	1.12E-05 (−0.005 to 0.005)	0.996	0.001 (−0.007 to 0.008)	0.861
CMT, μm	0.001 (−0.006 to 0.003)	**<0.001***	0 (−0.001 to 0.000)	0.253	−7.26E-05 (−0.001 to 0.000)	0.760	−0.001 (−0.002 to 1.693E-5)	0.055
Ganglion cell layer, μm	0.001 (−0.001 to 0.000)	0.330	0.001 (−0.001 to 0.004)	0.187	0.001 (−0.001 to 0.004)	0.194	0.001 (−0.001 to 0.004)	0.422
vCD (%)	−0.026 (−0.001 to 0.004)	0.452	−0.029 (−0.075 to 0.018)	0.225	−0.023 (−0.069 to 0.023)	0.331	−0.010 (−0.084 to 0.065)	0.802
Average RNFL, μm	−0.001 (−0.075 to 0.018)	0.254	0 (−0.001 to 0.002)	0.769	0.000 (−0.001 to 0.002)	0.894	0.001 (−0.001 to 0.003)	0.427
Superior RNFL, μm	0 (−0.001 to 0.002)	0.983	0 (−0.001 to 0.000)	0.714	−6.13E-05 (−0.001 to 0.001)	0.833	0.000 (−0.001 to 0.001)	0.783
Inferior RNFL, μm	0.001 (−0.001 to 0.000)	0.048	0 (−0.001 to 0.001)	0.647	0.000 (−0.001 to 0.001)	0.488	0.000 (−0.001 to 0.001)	0.821
Degree of lens dislocation (%) (severe)	0.029 (−0.001 to 0.001)	0.400	−0.008 (−0.058 to 0.042)	0.747	−0.003 (−0.050 to 0.044)	0.904	0.040 (−0.033 to 0.114)	0.282
Aortic diameter sinuses of Valsalva, mm	0.004 (−0.008 to 0.000)	0.074	−0.004 (−0.008 to 0.000)	0.057	−0.003 (−0.007 to 0.001)	0.143	−0.003 (−0.009 to 0.002)	0.260

(*continued on next page*)

Table 5. (*Continued*)

	Central PD		Parafoveal PD		Full-Area PD		Paranasal-Area PD	
	β (95% CI)	*P*	β (95% CI)	*P*	β (95% CI)	*P*	β (95% CI)	*P*
Z score	−0.003 (0.000 to 0.002)	0.589	0.013 (0.001 to 0.025)	0.034	0.011 (−0.001 to 0.023)	0.069	0.007 (−0.007 to 0.022)	0.310
EF	0.001 (−0.001 to 0.003)	0.219	0.001 (0.000 to 0.002)	0.155	0.001 (0.000 to 0.002)	0.137	0.000 (−0.001 to 0.002)	0.597

	Paratemporal-Area PD		Parasuperior-Area PD		Parainferior-Area PD	
	β (95% CI)	*P*	β (95% CI)	*P*	β (95% CI)	*P*
Age, years	0.001 (−0.003 to 0.006)	0.556	0.004 (−0.002 to 0.010)	0.231	0.001 (−0.006 to 0.007)	0.863
Sex (male%)	−0.034 (−0.054 to −0.014)	**0.001***	−0.023 (−0.052 to 0.007)	0.134	−0.018 (−0.051 to 0.014)	0.270
BCVA (logMAR [Snellen])	−0.016 (−0.042 to 0.010)	0.238	0.01 (−0.029 to 0.048)	0.629	−0.051 (−0.095 to −0.008)	0.020
SE, D	−0.001 (−0.002 to 2.562E-5)	0.055	−0.002 (−0.004 to 0.000)	0.078	0.001 (−0.001 to 0.002)	0.530
Intraocular pressure, mmHg	0.002 (−0.001 to 0.004)	0.226	0.000 (−0.004 to 0.004)	0.945	−0.001 (−0.004 to 0.003)	0.708
AL, mm	−0.004 (−0.008 to 0.001)	0.086	0.001 (−0.006 to 0.008)	0.793	−0.003 (−0.009 to 0.003)	0.300
CMT, μm	−0.001 (−0.001 to −9.281E-5)	0.020	0.000 (−0.001 to 0.001)	0.483	−0.001 (−0.002 to 0.000)	0.106
Ganglion cell layer, μm	0.002 (0.000 to 0.003)	0.076	0.002 (−8.743E-5 to 0.004)	0.061	0.001 (−0.001 to 0.004)	0.300
vCD (%)	−0.007 (−0.061 to 0.048)	0.812	−0.058 (−0.136 to 0.020)	0.146	−0.048 (−0.127 to 0.031)	0.234
Average RNFL, μm	0.000 (−0.001 to 0.002)	0.850	0.001 (−0.002 to 0.003)	0.696	−0.001 (−0.003 to 0.002)	0.663
Superior RNFL, μm	0.000 (−0.001 to 0.000)	0.476	0.000 (−0.001 to 0.001)	0.537	6.14E-05 (−0.001 to 0.001)	0.875
Inferior RNFL, μm	0.001 (0.000 to 0.001)	0.262	0.000 (−0.002 to 0.001)	0.658	0.001 (0.000 to 0.002)	0.156
Degree of lens dislocation (%) (severe)	−0.067 (−0.141 to 0.007)	0.075	−0.067 (−0.158 to 0.023)	0.145	0.039 (−0.057 to 0.135)	0.422
Aortic diameter sinuses of Valsalva, mm	−0.005 (−0.008 to −0.001)	0.016	−0.005 (−0.010 to 0.001)	0.091	−0.003 (−0.008 to 0.003)	0.358
Z score	0.020 (0.010 to 0.029)	<**0.001***	0.013 (−0.001 to 0.027)	0.064	0.010 (−0.005 to 0.025)	0.207
EF	0.002 (0.001 to 0.003)	**0.003***	0.000 (−0.001 to 0.002)	0.644	0.001 (−0.001 to 0.002)	0.497

**P* value significant after applying the corrected alpha threshold of 0.003. Bold indicates significant values.

Table 6. Correlations Between Baseline Characteristics and FAZ in MFS Patients Using Generalized Estimating Equations for Logistic Regression Analysis

	FAZ Area		FAZ Perimeter		FAZ Circularity Index	
	β (95% CI)	*P*	β (95% CI)	*P*	β (95% CI)	*P*
Age, years	0.021 (0.015 to 0.028)	<**0.001***	0.102 (0.054 to 0.149)	<**0.001***	0.004 (−0.015 to 0.022)	0.690
Sex (male%)	0.024 (−0.011 to 0.059)	0.186	0.017 (−0.179 to 0.212)	0.869	0.051 (−0.008 to 0.110)	0.090
BCVA (logMAR [Snellen])	−0.011 (−0.055 to 0.034)	0.633	0.160 (−0.141 to 0.462)	0.297	−0.065 (−0.203 to 0.074)	0.359
SE, D	−0.001 (−0.003 to 0.000)	0.146	−0.009 (−0.021 to 0.002)	0.119	0.001 (−0.002 to 0.005)	0.491
Intraocular pressure, mmHg	0.003 (−0.002 to 0.008)	0.230	0.021 (−0.021 to 0.062)	0.330	0.003 (−0.009 to 0.015)	0.602
AL, mm	−0.022 (−0.030 to −0.014)	<**0.001***	−0.096 (−0.153 to −0.039)	**0.001***	−0.013 (−0.027 to 0.002)	0.086
CMT, μm	−0.003 (−0.004 to −0.002)	<**0.001***	−0.017 (−0.023 to −0.011)	<**0.001***	0.002 (−0.001 to 0.004)	0.142
Ganglion cell layer, μm	−0.001 (−0.003 to 0.002)	0.582	−0.005 (−0.021 to 0.012)	0.585	0.002 (−0.002 to 0.006)	0.393
vCD (%)	−0.039 (−0.104 to 0.025)	0.233	0.015 (−0.470 to 0.500)	0.952	−0.211 (−0.402 to −0.019)	0.031
Average RNFL, μm	0.004 (0.001 to 0.007)	0.004	0.013 (−0.004 to 0.031)	0.131	0.004 (−0.001 to 0.010)	0.105
Superior RNFL, μm	−0.002 (−0.003 to −0.001)	0.005	−0.008 (−0.016 to 0.001)	0.074	−0.002 (−0.004 to 0.001)	0.173
Inferior RNFL, μm	−0.002 (−0.003 to 0.000)	0.011	−0.006 (−0.016 to 0.003)	0.191	−0.002 (−0.005 to 0.000)	0.075
Degree of lens dislocation (%) severe	0.028 (−0.090 to 0.145)	0.643	0.219 (−0.590 to 1.028)	0.596	−0.153 (−0.457 to 0.151)	0.323
Aortic diameter (sinuses of Valsalva, mm)	−0.011 (−0.018 to −0.005)	**0.001***	−0.038 (0.006 to 2.824)	0.093	−0.014 (−0.027 to −0.002)	0.020
Z score	0.024 (0.008 to 0.041)	0.004	0.060 (0.172 to 1.136)	0.286	0.039 (0.013 to 0.065)	**0.003***
EF	−0.001 (0.003 to 0.002)	0.684	−0.005 (−0.026 to 0.016)	0.645	0.004 (0.000 to 0.009)	0.073

**P* value significant after applying the corrected alpha threshold of 0.003. Bold indicates significant values.

dysfunction in patients with cardiovascular risk factors[18] and MFS patients have reduced rotational flow in the aorta and impaired function of left ventricle.[19] The results of our study reveal that patients with a larger ascending aorta diameter and left ventricular dysfunction correlates with impairment of retinal blood flow, which indicated that aortopathy in patients with MFS parallels retinal vascular defects. Indeed, despite the fact that severity of aortic disease is the most important diagnostic and prognostic factor determining outcome in this disease, accurate measurements are often difficult to obtain especially in children. Some echocardiographic parameters are affected by increased interobserver and intraexamination variability.[20] However, recent studies have shown a high repeatability and reproducibility of OCTA examination. An OCTA evaluation is easy to perform, objective, and complication free[21] and could be a promising biomarker supporting diagnosis or in providing prognostic information. In addition, retinal microvasculature has been proposed as an easily measured surrogate for systemic circulation. Previous studies in patients with congenital heart disease and coronary heart disease also found a decreased retinal VD compared with normal controls.[22]Therefore, the OCTA examination may provide a great future opportunity for the early recognition of cardiovascular damages in children with MFS.

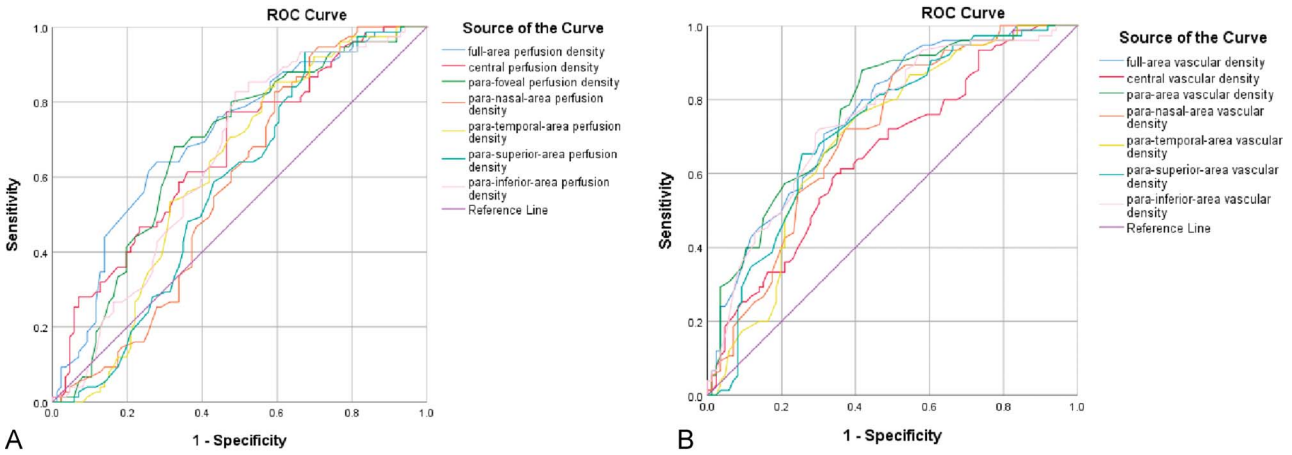

Fig. 2. Receiver operating characteristic curves of the OCTA-based parameters in the task of distinguishing the control eyes from the eyes with Marfan syndrome. **A.** Vascular density parameters. **B.** Perfusion density parameters.

Importantly, we found that central VD and PD were negatively correlated with BCVA. It has been shown that almost half of the MFS patients had amblyopia in spite of good conservative management.[23] Our finding suggests that the retinal PD and VD may correlate with the occurrence and development of visual outcomes in MFS patients. Visual acuity was found to be associated with FAZ circularity and vessel diameter index in amblyopic eyes and in patients with spontaneously regressed retinopathy of prematurity.[24] In diabetic retinopathy, decreased VD was also found to be associated with a reduction in the visual function.[25] Nevertheless, VD was not correlated with VA in normal children.[26] Therefore, whether foveal microvasculature itself or in combination with other parameters can contribute to the complex function of visual acuity remained to be investigated.

In this study, the reduction of macular central VD and central PD in MFS patients were also found to be positively correlated with the CMT, suggesting that changes in the vasculature network that supports the inner retina could lead to structural consequences. A previous study suggested that a reduction in the retinal blood supply to inner retinal neurons may cause cell death and ischemia.[27] At the same time, most OCT parameters were found to be correlated with OCTA parameters in healthy participants 5 to 80 years old.[28]

Finally, we found that the AL was correlated with the superficial vasculatures. In myopic eyes and many healthy controls, the retinal vessel density was reduced.[29] We and others confirmed that the superficial macular vessel density was higher in girls than in boys.[24] On the contrary, some studies found the opposite result.[23] More evidence is required to investigate the sex discrepancy in the retinal vessel density.

Microvascular alterations can be an early sign for certain diseases and correlated with functional parameters. It is worthy to note that the identification of early microvascular impairment may indicate which patients seem to have higher risk of developing cardiovascular diseases and should be more frequently monitored. To investigate how accurate the OCTA perimeters can be in the diagnosis of children with MFS, we examined 14 different potentially discriminatory features. We found that the para-area VD (AUC: 770) had the best diagnostic efficacy in distinguishing a healthy eye from an MFS one; however, the diagnostic value of this finding needs to be determined in a larger sample study. Both large retinal vessels and capillaries build up the superficial retinal capillary network whose metrics had been showed to have a good diagnostic performance in systemic diseases such as diabetes mellitus, hypertension, and cardiovascular disease.[30] A future longitudinal study is required to investigate the cause-and-effect relationship between MFS and OCTA metrics and any such possible relationship.

The limitations of this study are that this is single-center study with monoracial background (all subjects were from China), a relatively small sample size, and a lack of long-term follow-up, which may have increased the bias of the study. More extensive and longitudinal studies are necessary to verify these results.

This study confirmed that young MFS patients have morphological changes in the macular microvasculature. Alterations of microvascular flow were associated with visual acuity, CMT, aorta size, Z-score, and EF, suggesting that the inner retina of MFS patients had vascular changes which were structurally, functionally and systemically associated with MFS. In general, our results highlight the capability of OCTA to accurately characterize retinal microvascular network changes in MFS patients enabling further understanding of the pathogenesis of arterial disease in MFS. Therefore, OCTA and quantitative OCTA metrics, such as VD,

PD, and FAZ, could be a reliable, objective, and automated tool in the recognition and evaluation of MFS. Further randomized trials with larger patient groups and additional systemic parameters could shed more light on this issue.

Key words: foveal microvasculature, Marfan syndrome, optical coherence tomography angiography.

Acknowledgments

The authors thank Ms. Ling Jin for useful suggestions in revising the manuscript.

References

1. Judge DP, Dietz HC. Marfan's syndrome. Lancet 2005;366: 1965–1976.
2. Izquierdo NJ, Traboulsi EI, Enger C, Maumenee IH. Glaucoma in the Marfan syndrome. Trans Am Ophthalmol Soc 1992;90: 111–117.
3. Lee B, Godfrey M, Vitale E, et al. Linkage of Marfan syndrome and a phenotypically related disorder to two different fibrillin genes. Nature 1991;352:330–334.
4. Patton N, Aslam T, Macgillivray T, et al. Retinal vascular image analysis as a potential screening tool for cerebrovascular disease: a rationale based on homology between cerebral and retinal microvasculatures. J Anat 2005;206:319–348.
5. Wong TY, Klein R, Klein BE, et al. Retinal microvascular abnormalities and their relationship with hypertension, cardiovascular disease, and mortality. Surv Ophthalmol 2001;46:59–80.
6. Hoffman RS, Snyder ME, Devgan U, et al. Management of the subluxated crystalline lens. J Cataract Refract Surg 2013;39: 1904–1915.
7. Al-Sheikh M, Falavarjani KG, Akil H, Sadda SR. Impact of image quality on OCT angiography based quantitative measurements. Int J Retina Vitreous 2017;3:13.
8. Baumgartner H, Bonhoeffer P, Groot NM, et al. ESC Guidelines for the management of grown-up congenital heart disease (new version 2010). Eur Heart J 2010;31:2915–2957.
9. Colan SD, McElhinney DB, Crawford EC, et al. Validation and re-evaluation of a discriminant model predicting anatomic suitability for biventricular repair in neonates with aortic stenosis. J Am Coll Cardiol 2006;47:1858–1865.
10. van Kimmenade RR, Kempers M, de Boer MJ, et al. A clinical appraisal of different Z-score equations for aortic root assessment in the diagnostic evaluation of Marfan syndrome. Genet Med 2013;15:528–532.
11. DeLong ER, DeLong DM, Clarke-Pearson DL. Comparing the areas under two or more correlated receiver operating characteristic curves: a nonparametric approach. Biometrics 1988;44:837–845.
12. Awais M, Williams DM, Deeb GM, Shea MJ. Aneurysms of medium-sized arteries in Marfan syndrome. Ann Vasc Surg 2013;27:1188.e5–1188.e7.
13. Eberth JF, Taucer AI, Wilson E, Humphrey JD. Mechanics of carotid arteries in a mouse model of Marfan Syndrome. Ann Biomed Eng 2009;37:1093–1104.
14. Cao Q, Xiao B, Jin GM, et al. Expression of transforming growth factor beta and matrix metalloproteinases in the aqueous humor of patients with congenital ectopia lentis. Mol Med Rep 2019;20:559–566.
15. Takata M, Amiya E, Watanabe M, et al. Impairment of flow-mediated dilation correlates with aortic dilation in patients with Marfan syndrome. Heart Vessels 2014;29:478–485.
16. Grillo A, Salvi P, Marelli S, et al. Impaired central pulsatile hemodynamics in children and adolescents with Marfan syndrome. J Am Heart Assoc 2017;6:e006815.
17. Sandor GG, Hishitani T, Petty RE, et al. A novel Doppler echocardiographic method of measuring the biophysical properties of the aorta in pediatric patients. J Am Soc Echocardiogr 2003;16:745–750.
18. Masugata H, Senda S, Murao K, et al. Aortic root dilatation as a marker of subclinical left ventricular diastolic dysfunction in patients with cardiovascular risk factors. J Int Med Res 2011;39:64–70.
19. De Backer JF, Devos D, Segers P, et al. Primary impairment of left ventricular function in Marfan syndrome. Int J Cardiol 2006;112:353–358.
20. Morbach C, Gelbrich G, Breunig M, et al. Impact of acquisition and interpretation on total inter-observer variability in echocardiography: results from the quality assurance program of the STAAB cohort study. Int J Cardiovasc Imaging 2018; 34:1057–1065.
21. Coscas F, Sellam A, Bernard AG, et al. Normative data for vascular density in superficial and deep capillary plexuses of healthy adults assessed by optical coherence tomography angiography. Invest Ophthalmol Vis Sci 2016;57:OCT211–OCT223.
22. Li C, Zhong P, Yuan H, et al. Retinal microvasculature impairment in patients with congenital heart disease investigated by optical coherence tomography angiography. Clin Exp Ophthalmol 2020;48:1219–1228.
23. Romano PE, Kerr NC, Hope GM. Bilateral ametropic functional amblyopia in genetic ectopia lentis: its relation to the amount of subluxation, an indicator for early surgical management. Binocul Vis Strabismus Q 2002;17:235–241.
24. Wong ES, Zhang XJ, Yuan N, et al. Association of optical coherence tomography angiography metrics with detection of impaired macular microvasculature and decreased vision in amblyopic eyes: the Hong Kong children eye study. JAMA Ophthalmol 2020;138:858–865.
25. Lee MW, Lee WH, Ryu CK, et al. Effects of prolonged type 2 diabetes on the inner retinal layer and macular microvasculature: an optical coherence tomography angiography study. J Clin Med 2020;9:1849.
26. Cheung CY, Li J, Yuan N, et al. Quantitative retinal microvasculature in children using swept-source optical coherence tomography: the Hong Kong Children Eye Study. Br J Ophthalmol 2018. Epub ahead of print.
27. Trinh M, Kalloniatis M, Nivison-Smith L. Vascular changes in intermediate age-related macular degeneration quantified using optical coherence tomography angiography. Transl Vis Sci Technol 2019;8:20.
28. Tiryaki Demir S, Kiray Bas E, Karapapak M, et al. Effect of prematurity on foveal development in early school-age children. Am J Ophthalmol 2020;219:177–185.
29. You QS, Chan JC, Ng AL, et al. Macular vessel density measured with optical coherence tomography angiography and its associations in a large population-based study. Invest Ophthalmol Vis Sci 2019;60:4830–4837.
30. Drobnjak D, Munch IC, Glümer C, et al. Retinal vessel diameters and their relationship with cardiovascular risk and all-cause mortality in the Inter99 eye study: a 15-year follow-up. J Ophthalmol 2016;2016:6138659.